Journal of Solid State Chemistry **163**, 308–312 (2002)
doi:10.1006/jssc.2001.9416, available online at http://www.idealibrary.com on IDEAL®

A Lead Molybdenum(V) Monophosphate with a Tunnel Structure: $Pb_3(MoO)_3(PO_4)_5$

A. Leclaire, J. Chardon, J. Provost, and B. Raveau

Laboratoire CRISMAT, UMR CNRS ISMRA 6508, 6 bd Maréchal Juin, 14050 Caen Cedex, France

Received July 17, 2001; in revised form September 26, 2001; accepted September 28, 2001

A molybdenum(V) monophosphate containing lead has been synthesized for the first time. This new phase $Pb_3(MoO)_3(PO_4)_5$ crystallizes in the *Pnma* space group with $a = 14.280(1)$ Å, $b = 15.679(1)$ Å, and $c = 8.129(1)$ Å. The crystal structure was refined up to $R = 0.0406$ and $R_w = 0.0446$. The original three-dimensionnal framework of this compound, $[Mo_3P_5O_{23}]_\infty$, can be described by the assemblage of $[Mo_3P_5O_{28}]_\infty$ ribbons running along $\vec{b}$ and forming elliptic tunnels where the Pb^{2+} cations are located. The topological analogy of this structure with aeschynite is emphasized. The stereoactivity of the $6s^2$ lone pair of Pb^{2+} is discussed. © 2002 Elsevier Science

INTRODUCTION

The association of transition metal elements with phosphate and silicate frameworks has made it possible to synthesize a huge number of opened structures. This is, for example, the case with the molybdenum(V) phosphates obtained either by hydrothermal methods (1) or by solid state reaction (2). Starting from the earlier investigations of the univalent Mo(V) phosphates (3–7), a huge number of new frameworks have been discovered. Nevertheless, only a few divalent Mo(V) phosphates are actually known, three of them containing barium (8–10) and one containing cadmium (11). Considering the possibility of introducing lead in molybdenophosphate matrices, it appears that only one molybdenum(VI) monophosphate, $Pb(MoO_2)_2PO_4$, has been synthesized by Masse *et al.* (12), but no reduced molybdenum phosphate containing lead is known to date. We have thus revisited the Pb–Mo–P–O system, taking into consideration for molybdenum a reduced valency. We report herein on the synthesis and structure of the first lead molybdenum(V) monophosphate, $Pb_3(MoO)_3(PO_4)_5$.

Crystal Growth and Synthesis

Single crystals of the title compound were grown from a mixture of nominal composition $Pb_2P_4Mo_2O_{17}$. First $PbCO_3$, $H(NH_4)_2PO_4$, and MoO_3 were mixed in an agate mortar in the molar ratios 2:4:1.6667 and heated at 600 K in a platinum crucible to decompose the ammonium phosphate and the carbonate. In a second step the resulting mixture was crushed, added to metallic molybdenum powder, i.e., to 0.333Mo and to 2% weight of $PbBr_2$, and sealed in an evacuated silica ampoule, and then heated for 12 hrs at 813 K and cooled at 3.5 K per hour to 473 K and finally quenched to room temperature. Beautiful green crystals were extracted from a black product.

The pure phase is also obtained with a similar two-step process. First a mixture of $PbCO_3$, $H(NH_4)_2PO_3$, and MoO_3 with the molar ratios 3:5:2.5 is heated at 600 K. The resulting mixture is added to metallic molybdenum powder (0.5Mo) and sealed in an evacuated silica ampoule, and then heated for 12 hrs at 923 K and cooled in the same way as the previous process.

The X-ray powder diffraction film of the resulting green product fits well to the one calculated from the atomic parameters obtained by single-crystal X-ray study.

Crystal Structure Determination

A light green crystal with dimensions $0.154 \times 0.077 \times 0.013$ mm was selected for the structure determination after tests made with film techniques on a Weissenberg camera. The cell parameters (Table 1) were determined with a least-squares method using 25 reflections with $18° < \theta < 22°$. The data were recorded at room temperature on an Enraf-Nonius CAD 4 diffractometer using Mo$K\alpha$ radiation ($\lambda = 0.71073$ Å) isolated with a graphite monochromator. Intensities were checked by monitoring three standard reflections every hour. No significant deviations in intensities were observed. The intensity data were corrected for the Lorentz polarization and absorption and secondary extinction effects. The absorption corrections were computed by the gaussian method using the shape of the crystal. The systematic absences $k + l = 2n + 1$ in $0kl$ and $h = 2n + 1$ in $hk0$ are consistent with the *Pnma* (62) and the $Pn2_1a$ (33) space groups. The Harker line 0V0 observed on the

0022-4596/02 $35.00
© 2002 Elsevier Science
All rights reserved.

TABLE 1
Summary of Crystal Data, Intensity Measurement, and Structure Refinement for $Pb_3(MoO)_3(PO_4)_5$

Chemical formula	$Pb_3Mo_3P_5O_{23}$
Molecular weight	1429.24D
Crystal system	Orthorhombic
Space group	*Pnma* (62)
Cell dimensions	$a = 14.280(1)$ Å
	$b = 15.6788(8)$ Å
	$c = 8.1291(7)$ Å
Cell volume	1820.0(2) Å^3
Z	4
Density	5.22
μ (mm^{-1})	30.24
$T_{min.}$	0.1724
$T_{max.}$	0.5557
Secondary extinction	0.331(8)
Measured reflections	7659
Reflections with $I > 3\sigma(I)$	1458
Temperature of the data collections	21°C
Number of variables	113
R (F_o)	0.0406
R_W	0.0446

Patterson function is characteristic of the centrosymmetric space group *Pnma* (62).

The structure was solved with the heavy atom method. The full-matrix least-squares refinements were performed on F weighted by $1/\sigma(F)^2$ with the JANA98 package (13). The latter lead to $R = 0.0406$ and $R_w = 0.0446$ and to the atomic parameters given in Table 2.

TABLE 2
Atomic Coordinates and Thermal Factors of $Pb_3(MoO)_3(PO_4)_5$

Atom	x	y	z	U_{eq} (Å^2)
Pb(1)	0.09799(3)	0.08380(7)	0.04418(8)	0.0134(1)
Pb(2)	0.11000(5)	0.75	0.0483(2)	0.0139(3)
Mo(1)	0.65209(6)	0.4168(1)	− 0.0053(1)	0.0071(2)
Mo(2)	0.3455(1)	0.25	0.0574(2)	0.0063(4)
P(1)	0.5629(2)	0.5947(3)	0.1790(5)	0.009(1)
P(2)	0.8548(2)	0.4286(2)	0.2135(4)	0.0052(9)
P(3)	0.5675(4)	0.25	0.2009(8)	0.008(1)
O(1)	0.6880(6)	0.3471(7)	− 0.145(2)	0.022(3)
O(2)	0.6300(6)	0.3314(6)	0.179(1)	0.009(2)
O(3)	0.7816(5)	0.4442(6)	0.079(1)	0.011(2)
O(4)	0.5158(5)	0.4150(9)	− 0.057(1)	0.012(2)
O(5)	0.6730(6)	0.5253(6)	− 0.129(1)	0.012(2)
O(6)	0.6124(6)	0.5084(6)	0.199(1)	0.008(2)
O(7)	0.2296(9)	0.25	0.032(3)	0.032(6)
O(8)	0.3654(6)	0.3395(7)	− 0.116(1)	0.015(2)
O(9)	0.3566(6)	0.1684(6)	0.251(1)	0.012(2)
O(10)	0.4916(9)	0.25	0.068(3)	0.014(3)
O(11)	0.5263(6)	0.6287(6)	0.344(1)	0.012(2)
O(12)	0.9475(6)	0.4586(6)	0.143(1)	0.009(2)
O(13)	0.5327(9)	0.25	0.380(2)	0.013(3)

DESCRIPTION OF THE STRUCTURE AND DISCUSSION

The structure determination of this new phase shows that it possesses a three-dimensional framework of corner-sharing MoO_6 octahedra and PO_4 tetrahedra, so it can be formulated as a Mo(V) monophosphate $Pb_3(MoO)_3(PO_4)_5$. The projection of the structure of this compound along $\vec{b}$ (Fig. 1) shows that the $[Mo_3P_5O_{23}]_\infty$ framework delimits large elliptic tunnels (maximum size ≈ 10 Å) running along $\vec{b}$, where the lead cations are located. An important characteristic of this framework concerns the fact that each polyhedron has one free apex; i.e., each PO_4 tetrahedron shares only three corners with MoO_6 octahedra, whereas each MoO_6 octahedron shares only five corners with PO_4 tetrahedra. The free apices of these polyhedra form the walls of the elliptic tunnels.

The complex geometry of the $[Mo_3P_5O_{23}]_\infty$ framework is rather difficult to describe from other projections of the structure. Nevertheless, the projection along $\vec{c}$ (Fig. 2) shows that $[MoPO_8]_\infty$ chains run along $\vec{b}$ in which one MoO_6 octahedron alternates with one PO_4 tetrahedron. Such a feature is observed in many molybdenum and vanadium phosphates (2, 14). From the latter projection it can also be seen that the structure consists of $[Mo_2P_4O_{20}]_\infty$ layers parallel to (010) interconnected by $MoPO_9$ units. The geometry of the $[Mo_2P_4O_{20}]_\infty$ layers, forming elliptic rings where two Pb(1) cations are sitting, can easily be seen from the projection of the structure along $\vec{b}$ (Fig. 1). More importantly, a detailed analysis of the structure allows the entire $[Mo_3P_5O_{23}]_\infty$ framework to be described by the assemblage of double $[Mo_3P_5O_{25}]_\infty$ ribbons running along $\vec{b}$ (Fig. 3). Such double ribbons are built up from two single $[Mo_3P_5O_{28}]_\infty$ ribbons in which a pair of PO_4 tetrahedra or

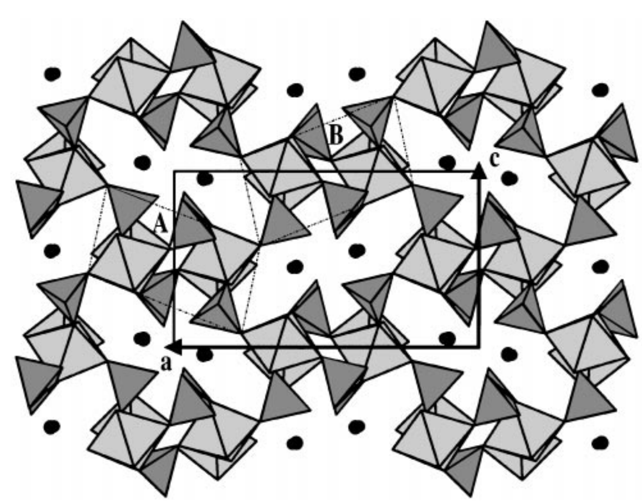

FIG. 1. Projection of the structure of $Pb_3(MoO)_3(PO_4)_5$ along $\vec{b}$ showing the tunnels containing the Pb atoms, and the two kinds (A and B) of $[Mo_3P_5O_{28}]_\infty$ ribbons.

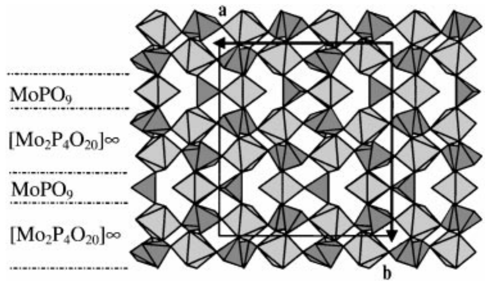

FIG. 2. Projection of the structure of $Pb_3(MoO)_3(PO_4)_5$ along $\vec{c}$ showing the stacking of the $[Mo_2P_4O_{20}]_\infty$ layers connected through the $MoPO_9$ units.

a single PO_4 tetrahedron alternates with one MoO_6 octahedron along $\vec{b}$, as described in Fig. 3. Those double ribbons have the basal plane of their MoO_6 octahedra oriented either parallel to $(\bar{5}01)$ (labelled A in Fig. 1) or parallel to (501) (labelled B in Fig. 1). In fact, these two orientations correspond to a simple rotation of 180° around $\vec{a}$ of one ribbon with respect to the other. Along $\vec{c}$, these ribbons keep the same orientation, forming (100) slices in which identically oriented $[Mo_3P_5O_{28}]_\infty$ ribbons are interleaved with Pb^{2+} ribbons. As a consequence the $[Mo_3P_5O_{23}]_\infty$ frameworks consist of A-oriented slices alternating with B-oriented slices along $\vec{a}$ (Fig. 4a). In this description, two adjacent A- and B-oriented ribbons share the apices of their polyhedra in such a way that a tetrahedron of one A ribbon is connected to an octahedron of the adjacent B ribbon and vice versa. The topology of this structure (Fig. 4a) is remarkably similar to that of the aeschynite $CaTa_2O_6$ (15), (Fig. 4b): the double ribbons $[Mo_3P_5O_{28}]_\infty$ (labelled A or B) correspond to the double rows of TaO_6 octahedra in the aeschynite, forming similarly oriented tunnels occupied by Pb^{2+} and Ca^{2+} cations in this phosphate and in the aeschynite, respectively.

The geometry of the MoO_6 octahedra is characteristic of pentavalent molybdenum, with one short molybdenyl bond (1.66–1.67 Å) opposed to one abnormally long Mo–O bond (2.09–2.26 Å), the four equatorial Mo–O distances being intermediate, as shown in Table 3. The PO_4 tetrahedra are almost regular, with P–O bond lengths correlated to the nature of the bonds formed by the oxygen atom with the other cations of the structure (Table 3).

The environment of lead is very different for the two kinds of sites. For Pb(2), all the oxygen atoms are located on the same side with respect to lead (Fig. 5a), showing for this cation a rather strong stereoactivity. This feature is also supported by the fact that the three oxygen atoms O(11) and O(13) are located at very short distances (2.41–2.45 Å) (see

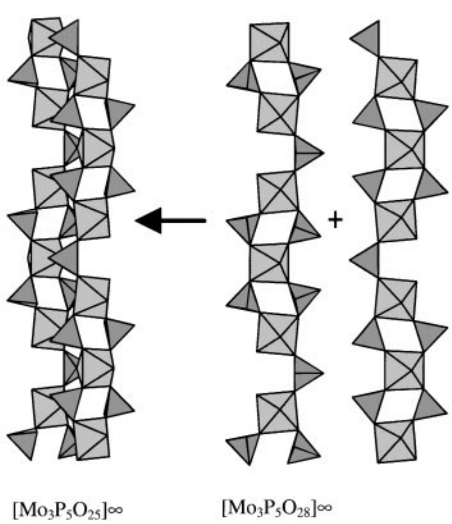

FIG. 3. The $[Mo_3P_5O_{25}]_\infty$ ribbons built up from two $[Mo_3P_5O_{28}]_\infty$ chains sharing some corners.

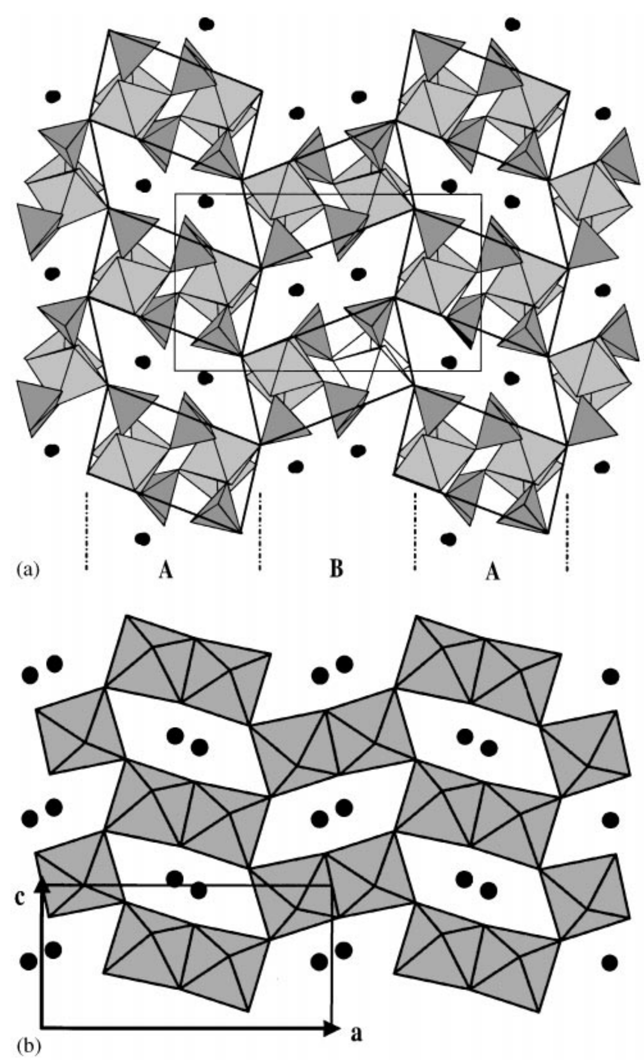

FIG. 4. (a) The stacking of the $[Mo_3P_5O_{25}]_\infty$ ribbon leading to a aeschynite-like framework. (b) The, aeschynite ($CaTa_2O_6$) frameworks.

TABLE 3
Interatomic Distance (Å) and Angle (°) in $Pb_3(MoO)_3(PO_4)_5$

Mo(1)	O(1)	O(2)	O(3)	O(4)	O(5)	O(6)
O(1)	1.66(1)	2.77(2)	2.72(2)	2.77(1)	2.81(1)	3.92(2)
O(2)	96.8(5)	2.034(9)	2.91(1)	2.84(1)	3.99(2)	2.79(1)
O(3)	95.1(4)	91.8(4)	2.019(7)	3.98(2)	2.62(1)	2.79(1)
O(4)	98.5(5)	89.7(4)	166.0(4)	1.991(7)	2.89(1)	2.89(1)
O(5)	99.8(5)	162.6(4)	81.5(4)	93.0(4)	1.999(9)	2.82(1)
O(6)	175.4(5)	80.7(3)	81.1(3)	85.4(4)	82.3(3)	2.268(9)
Mo(2)	O(7)	O(8)	O(8^{i})	O(9)	O(9^{i})	O(10)
O(7)	1.67(1)	2.68(2)	2.68(2)	2.85(2)	2.85(2)	3.75(2)
O(8)	93.1(7)	2.009(9)	2.81(2)	4.01(2)	2.99(1)	2.73(2)
O(8^{i})	93.1(7)	88.6(4)	2.009(9)	2.99(1)	4.01(2)	2.73(2)
O(9)	100.0(7)	166.2(4)	95.3(4)	2.034(9)	2.56(1)	2.75(2)
O(9^{i})	100.0(7)	95.3(4)	166.2(4)	77.9(4)	2.034(9)	2.75(2)
O(10)	175.3(9)	83.6(5)	83.6(5)	83.7(6)	73.7(6)	2.09(1)
P(1)	O(4^{ii})	O(6)	O(8^{ii})	O(11)		
O(4^{ii})	1.507(8)	2.48(1)	2.50(1)	2.50(1)		
O(6)	108.9(7)	1.54(1)	2.50(1)	2.54(1)		
O(8^{ii})	110.2(6)	108.6(5)	1.54(1)	2.46(1)		
O(11)	110.9(5)	111.7(5)	106.5(6)	1.535(9)		
P(2)	O(3)	O(5^{iii})	O(9^{iv})	O(12)		
O(3)	1.532(8)	2.51(1)	2.48(1)	2.44(1)		
O(5^{iii})	110.3(5)	1.523(9)	2.49(1)	2.54(1)		
O(9^{iv})	107.5(5)	108.3(5)	1.548(9)	2.56(1)		
O(12)	106.0(5)	113.4(5)	111.1(5)	1.517(9)		
P(3)	O(2)	O(2^{i})	O(10)	O(13)		
O(2)	1.568(9)	2.55(1)	2.52(2)	2.50(2)		
O(2^{i})	109.0(6)	1.568(9)	2.52(2)	2.50(2)		
O(10)	108.9(6)	108.9(6)	1.53(2)	2.60(2)		
O(13)	106.9(5)	106.9(5)	116.1(9)	1.54(2)		

Note. The *M*–O distances are on the diagonal and the O … O distances above it and the O–*M*–O angle under it.

Table 4), forming possibly with the $6s^2$ lone pair of Pb^{2+} a tetrahedron (Fig. 5a). The coordination of Pb(1) is less dissymmetric (Fig. 5b). Nevertheless, the $6s^2$ lone pair of this cation is still stereoactive, since all the oxygen atoms are located on the same side with respect to Pb(2), if one excepts O(7) which is located farther away at 3.21 Å. Note also that the weaker lone pair effect in Pb(2) compared to Pb(1) is clearly evidenced from the Pb–O distances (Table 4): the first one exhibits three abnormally short Pb–O bonds, smaller than 2.50 Å, whereas the second one exhibits only one short Pb–O distance (2.38 Å).

Finally, it is worth pointing out that the calculated bond valence sums (Table 5) are in agreement with the formal charges deduced from the chemical formula. The molar magnetic susceptibility $X_m(T)$ has been measured by SQUID magnetometry for $4.5 < T < 300$ K under a magnetic field $B = 0.3$ T. The results are shown in Fig. 6. Except for the two points corresponding to the lowest temperature,

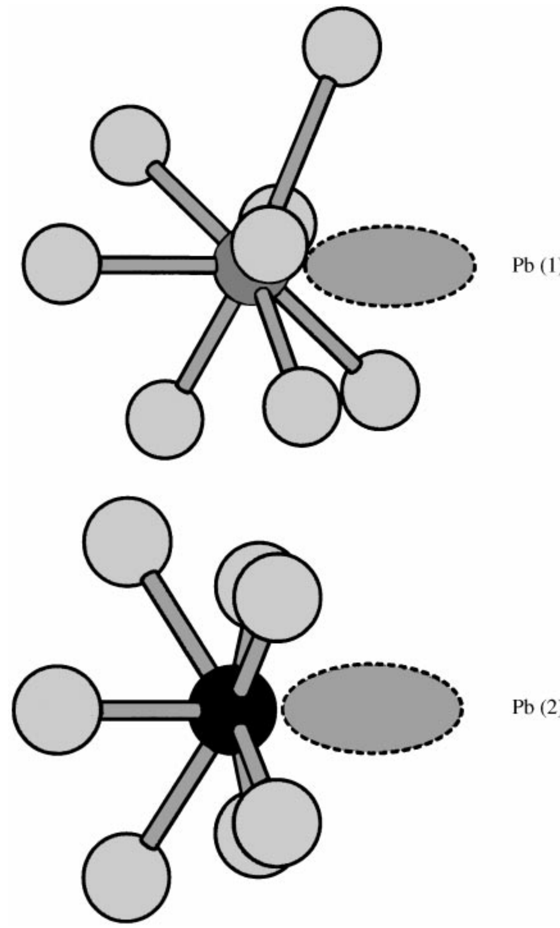

FIG. 5. The surrounding of the Pb atoms (a) $Pb(2)O_9$ and (b) $Pb(1)O_9$. The gray ellipse is the probable location of the lone pair of the lead.

TABLE 4
Lead Coordinations in $Pb_3(MoO)_3(PO_4)_5$

Pb(1)–O(12^{v})	2.389(9) Å
Pb(1)–O(11^{vi})	2.509(9) Å
Pb(1)–O(6^{vii})	2.548(9) Å
Pb(1)–O(12^{viii})	2.567(9) Å
Pb(1)–O(2^{vii})	2.653(9) Å
Pb(1)–O(13^{ix})	2.835(9) Å
Pb(1)–O(3^{x})	2.958(9) Å
Pb(1)–O(7)	3.214(8) Å
Pb(2)–O(11^{ix})	2.411(9) Å
Pb(2)–O(11^{xi})	2.411(9) Å
Pb(2)–O(13^{xii})	2.45(1) Å
Pb(2)–O(9^{xii})	2.776(9) Å
Pb(2)–O(9^{xiii})	2.776(9) Å
Pb(2)–O(8^{xiv})	3.089(9) Å
Pb(2)–O(8^{xv})	3.089(9) Å

Note. Symmetry codes. i: $x, \frac{1}{2} - y, z$. ii: $1 - x, 1 - y, -z$. iii: $\frac{3}{2} - x, 1 - y, \frac{1}{2} + z$. iv: $\frac{1}{2} + x, \frac{1}{2} - y, \frac{1}{2} - z$. v: $x - 1, \frac{1}{2} - y, + z$. vi: $\frac{1}{2} - x, y - \frac{1}{2}, z - \frac{1}{2}$. vii: $x - \frac{1}{2}, \frac{1}{2} - y, -z$. viii: $1 - x, \frac{1}{2} + y, -z$. ix: $x - \frac{1}{2}, y, \frac{1}{2} - z$. x: $1 - x, y - \frac{1}{2}, -z$. xi: $x - \frac{1}{2}, \frac{3}{2} - y, \frac{1}{2} - z$. xii: $\frac{1}{2} - x, 1 - y, z - \frac{1}{2}$. xiii: $\frac{1}{2} - x, \frac{1}{2} + y, z - \frac{1}{2}$. xiv: $\frac{1}{2} - x, 1 - y, \frac{1}{2} + z$. xv: $\frac{1}{2} - x, \frac{1}{2} + y, \frac{1}{2} + z$.

TABLE 5
Electrostatic Bond Valences in $Pb_3(MoO)_3(PO_4)_5$

	Mo(1)	Mo(2)	P(1)	P(2)	P(3)	Pb(1)	Pb(2)	Σve-
O(1)	2.000							2.000
O(2)	0.613				1.138	0.232		1.983
					1.138			
O(3)	0.648			1.247		0.102		1.997
O(4)	0.704		1.339					2.043
O(5)	0.689			1.280				1.969
O(6)	0.298		1.242			0.307		1.847
O(7)		1.926				0.051		1.977
O(8)		0.665	1.222				0.071	1.958
		0.665					0.071	
O(9)		0.612		1.200			0.167	1.979
		0.612					0.167	
O(10)		0.521			1.249			1.770
O(11)			1.245			0.342	0.446	2.033
							0.446	
O(12)				1.303		0.473/*0.292*		2.068
						0.292		
O(13)					1.219	0.142/*0.142*	0.399	1.902
Σve +	4.952	5.001	5.048	5.030	4.744	1.941	1.767	

Note. Due to the special position of some atoms the values in italics are used for the sums in the rows not in the columns. The second line in some rows is not used for the sums of this line but are used for the sums in the columns.

the experimental data fit very well with the standard Curie–Weiss law: $X_m = X_o + C/(T - \theta)$. The fitting Curie constant C leads to a magnetic moment of 1.69 μ_B per Mo(V). This value is in agreement with the theoritical value 1.73 μ_B expected for an isolated Mo^{5+} ion.

In conclusion, a Mo(V) phosphate containing lead has been obtained for the first time, showing that in this system Pb^{2+} is stable in the presence of Mo(V). This opens the route to the research of new lead molybdenum phosphates, involving a reduced state of molybdenum, especially Mo(V) and mixed-valent Mo(V)–Mo(VI). The analogy of this structure with aeschynite suggests that other mixed frameworks of transition metal phosphates with a topology similar to those of various pure octahedral structures should exist.

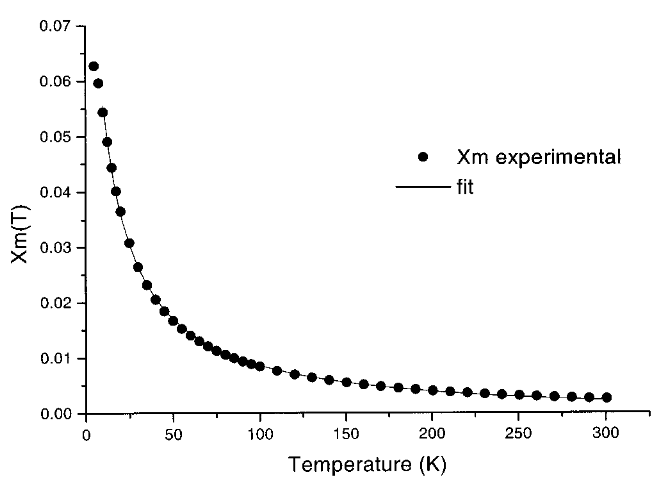

FIG. 6. The molar magnetic susceptibility $X_m(T)$ versus temperature T measured under $B = 0.3$ T. The black dots are experimental results and the solid line the fit with the Curie–Weiss law $X_m = X_o + C/(T - \theta)$.

REFERENCES

1. R. C. Haushalter and L. A. Mundi, *Chem. Mater*. **4,** 31 (1992).
2. G. Costentin, A. Leclaire, M. M. Borel, A. Grandin, and B. Raveau, *Rev. Inorg. Chem*. **13,** 77 (1993).
3. A. Leclaire, J. C. Monier, and B. Raveau, *J. Solid State Chem*. **48,** 147 (1983).
4. K. H. Lii and R. C. Haushalter, *J. Solid State Chem*. **69,** 320 (1987).
5. J. J. Chen, K. H. Lii, and S. L. Wang, *J. Solid State Chem*. **69,** 320 (1987).
6. A. Leclaire, M. M. Borel, A. Grandin, and B. Raveau, *Z. Kristallog*. **188,** 77 (1989).
7. R. C. Haushalter and F. W. Lai, *J. Solid State Chem*. **83,** 202 (1989).
8. G. Costentin, M. M. Borel, A. Grandin, A. Leclaire, and B. Raveau, *J. Solid State Chem*. **89,** 83 (1990).
9. M. M. Borel, J. Chardon, A. Leclaire, A. Grandin, and B. Raveau, *J. Solid State Chem*. **112,** 317 (1994).
10. S. Ledain, A. Leclaire, M. M. Borel, J. Provost, and B. Raveau, *J. Solid State Chem*. **125,** 147 (1991).
11. A. Guesdon, A. Leclaire, M. M. Borel, and B. Raveau, *J. Solid State Chem*. **122,** 343 (1996).
12. R. Masse, M. T. Averbuck-Ponchot, and A. Durif, *J. Solid State Chem*. **58,** 157 (1996).
13. V. Petricek and M. Dusek, JANA 98, Institute of Physics, Academy of Sciences of the Czech Republic, 1998.
14. S. Boudin, A. Guesdon, A. Leclaire, and M. M. Borel, *Int. J. Inorg*. Mater. **2,** 561 (2000).
15. L. Jahnberg, *Acta Chem. Scand*. **17,** 2548 (1963).